Electronic Supplementary Information

Plasmonics tunable Ag-coated gold nanorods arrays as reusable SERS substrates for multiplexed antibiotics detection

Xiaoya Peng, Dan Li *, Yuanting Li, Haibo Xing, Wei Deng

School of Chemical and Environmental Engineering, Shanghai Institute of Technology, 100 Haiquan Road, Shanghai 201418, PR China

* Corresponding author phone/fax: +86-21-60873241; E-mail: dany@sit.edu.cn (D. Li).

Raman Enhancement Factor. The Raman enhancement factor (EF) of the AgNPs/GNRs array was calculated as given in Eq. 1 from the literature [1, 2]:

$$\boldsymbol{EF = (I_{SERS} / I_{bulk}) \times (N_{bulk} / N_{SERS})} \tag{1}$$

where I_{SERS} and I_{bulk} are the vibration intensities in the SERS of 4-aminothiophenol (4-ATP) and normal Raman spectra of 4-ATP, respectively. N_{bulk} and $\boldsymbol{N}_{\mathrm{SERS}}$ are the number of molecules under laser illumination for the bulk sample, and the number of molecules in the self-assembled monolayers (SAMs), respectively. The N_{bulk} and $\boldsymbol{N}_{\mathrm{SERS}}$ values can be calculated based on the concentration of surface species or bulk sample and the corresponding sampling areas. It is reported that the average surface density of 4-ATP molecules in densely packed monolayers is approximately one 4-ATP molecule per 0.2 nm^2 [3]. Then the surface coverage of 4-ATP monolayer on AgNPs/GNRs array is 8.31×10^{-10} mol cm^{-2} (Γ=1 / [$(0.2\times10^{-14}) \times (6.02\times10^{23})$] mol cm^{-2}=8.31×10^{-10} mol cm^{-2}). Taking the sampling area (ca. 10 μm in diameter) into account, $\boldsymbol{N}_{\mathrm{SERS}}$ has a value of 6.52×10^{-16} mol ($\boldsymbol{N}_{\mathrm{SERS}} = \Gamma \times \pi \times (10/2)$ μm^2=6.52×10^{-16} mol). For the solid sample, the sampling volume is the product of the area of the laser spot (ca. 10 μm diameter) and the penetration depth (~ 2 μm) of the focused laser beam. Assuming the density of bulk 4-ATP is 1.18 g cm^{-3} [4, 5], N_{bulk} can be calculated to be 1.47×10^{-12} mol (N_{bulk}=1.18 g $cm^{-3} \times \pi \times 25$ $\mu m^2 \times 2$ μm / (125.19 g mol^{-1}) =1.47×10^{-12} mol). For the vibrational mode at 1080 cm^{-1}, the ratio of I_{SERS} to I_{bulk} was about 55.6, so EF was calculated to be 1. 26×10^{5} (55.6× [1.47×10^{-12}/ (6.52×10^{-16}) = 1.26×10^{5}).

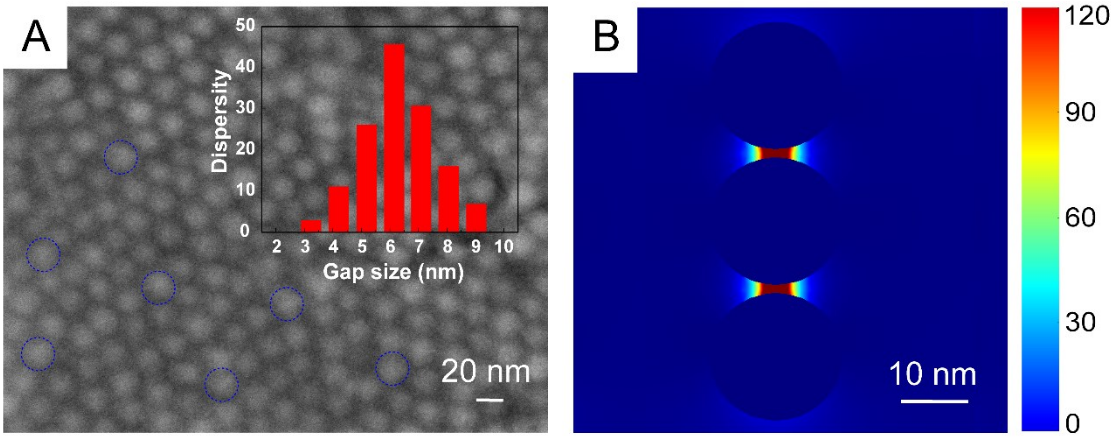

Fig. S1 (A) Top-view SEM image of AgNPs/GNR arrays with electrodeposition time of 2 min. The inset shows the pitch distribution of more than 120 GNRs from the AgNPs/GNRs array substrate. (B) The simulated near-field images of GNRs array substrate.

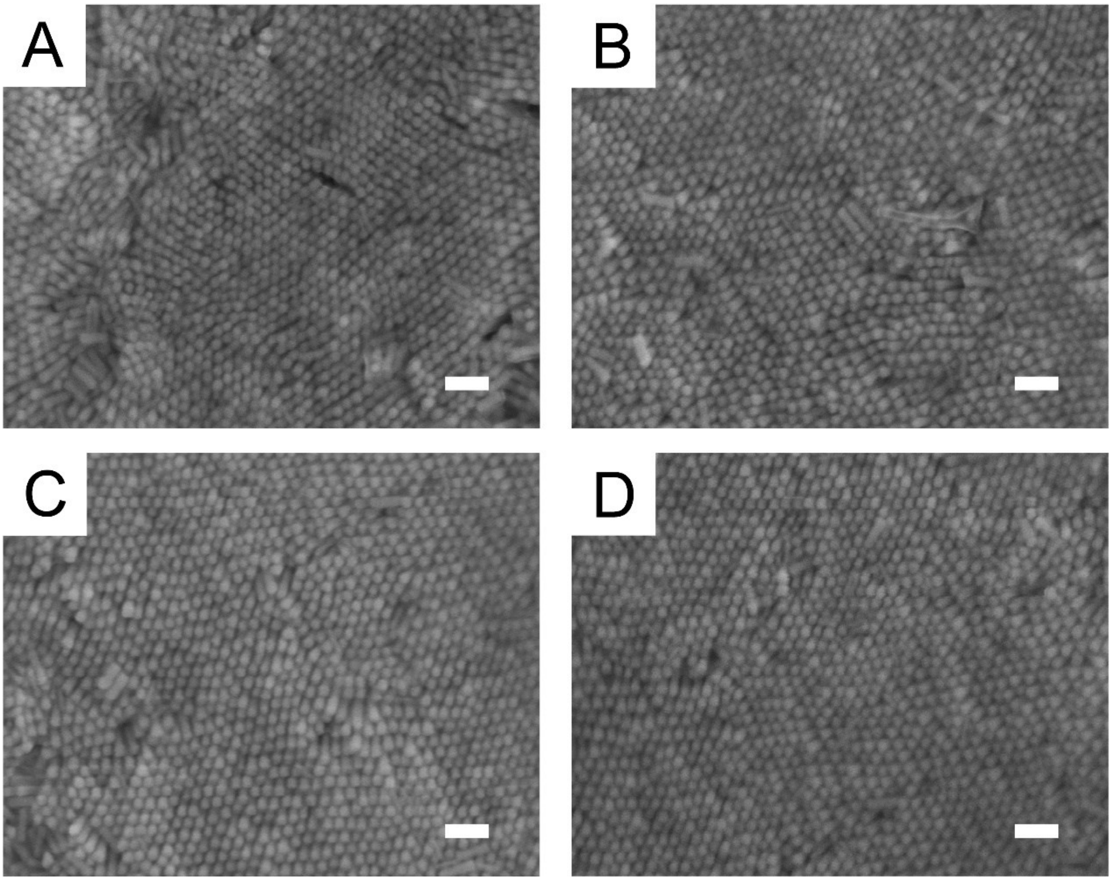

Fig. S2 SEM images of the (A) first, (B) second, (C) third and (D) fourth batch of AgNPs/GNR array substrates. Scale bar in A-D is 100 nm.

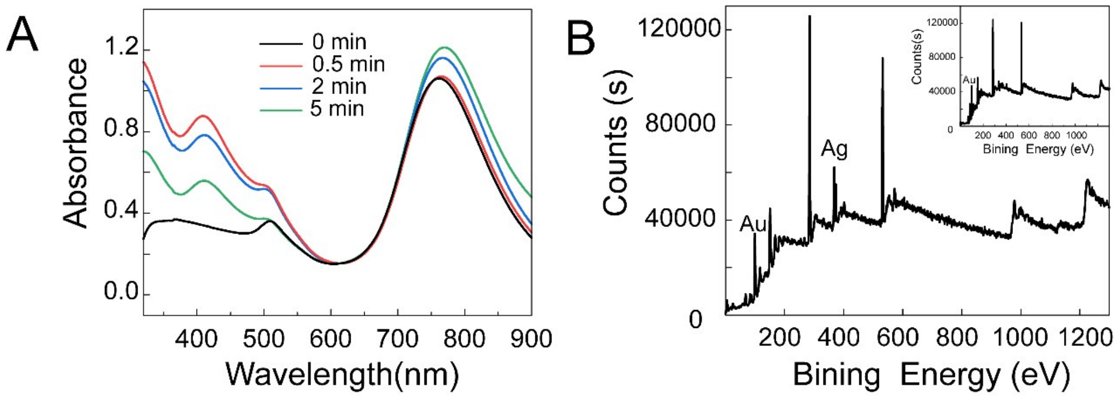

Fig. S3 (A) UV-Vis-NIR spectrum of the GNRs and AgNPs/GNRs array under different electrodeposition times. (B) XPS spectra of AgNPs/GNRs and GNRs arrays (inset).

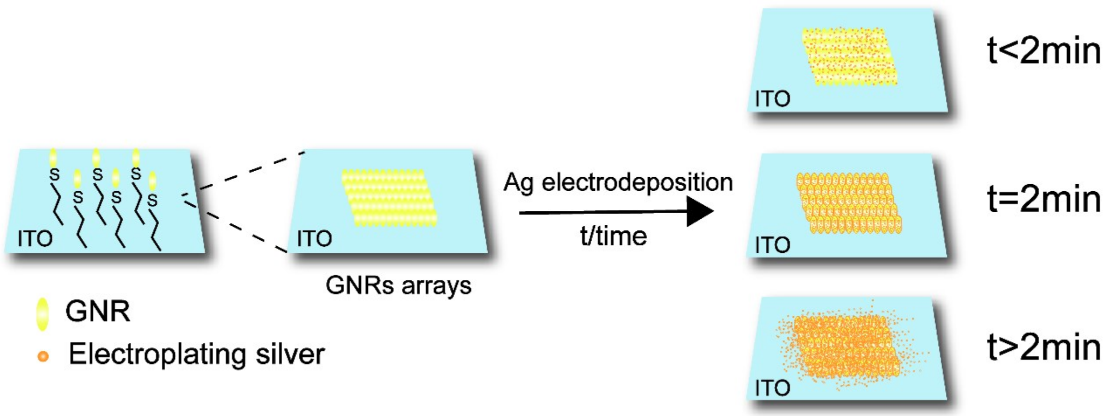

Fig. S4 The possible formation mechanism of the electrodeposition of Ag on the GNRs array under different electrodeposition time (t).

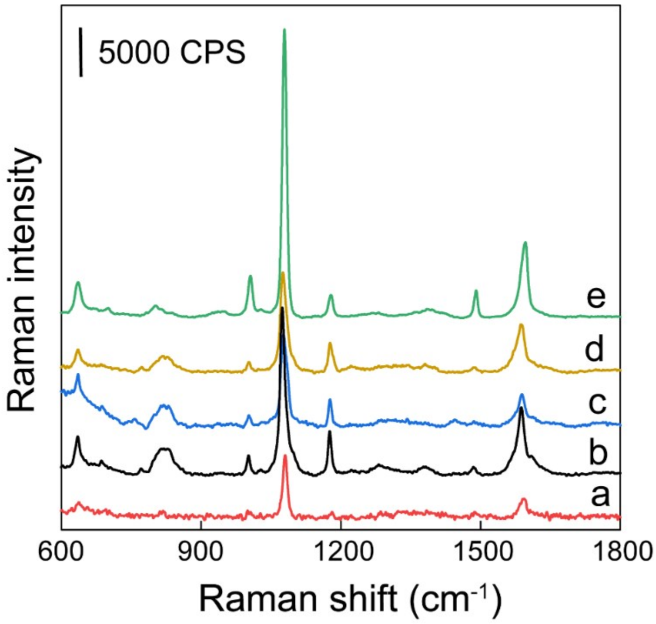

Fig. S5 SERS spectra of 4-ATP (1 μM) on AgNPs (a), GNRs (b), electrodeposited GNPs (c), electrodeposited AgNPs (d), and the AgNPs/GNRs array (e).

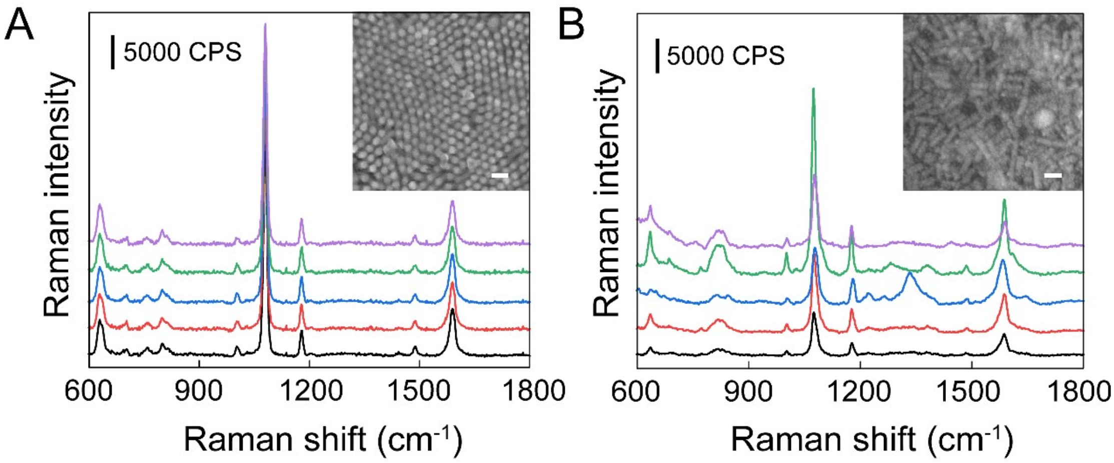

Fig. S6 SERS spectra of 4-ATP (1 μM) from 5 different spots on the same AgNPs/GNRs array (A) and disordered GNRs coated with electrodeposited silver (B). The insets display SEM images of AgNPs/GNRs array and randomly distributed GNRs coated with electrodeposited silver, respectively. Scale bar in insets is 50 nm.

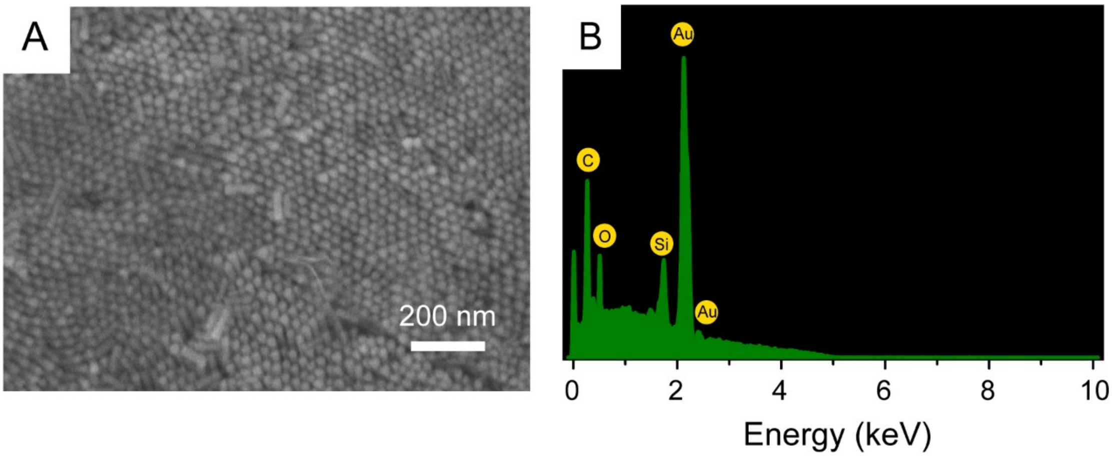

Fig. S7 (A) SEM image of the after stripped GNRs array, and (B) EDX elemental mapping of the after stripped GNRs array.

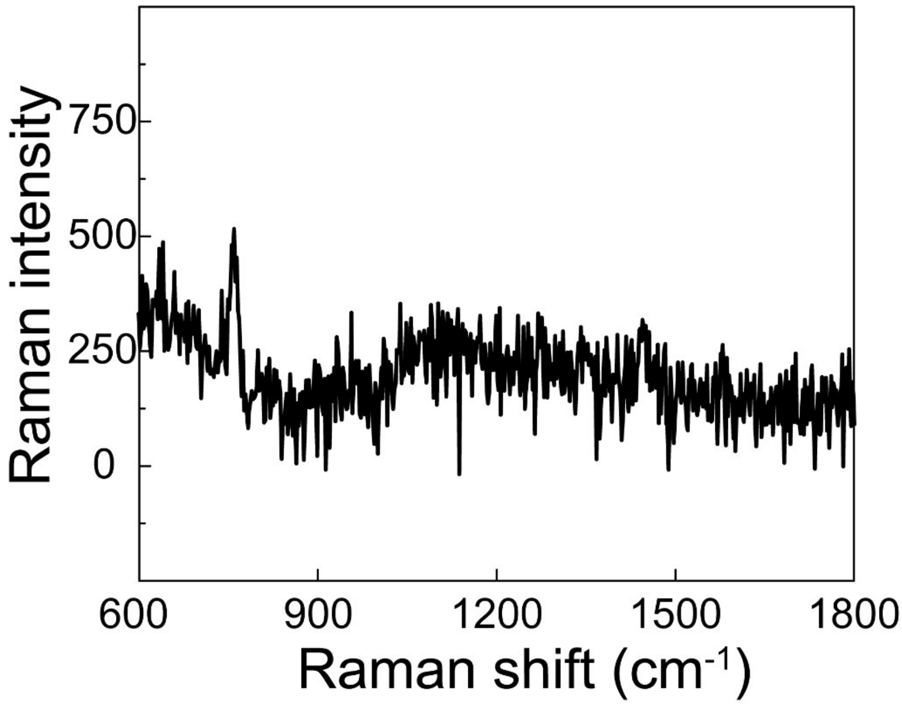

Fig. S8 Raman spectra of the AgNPs/GNRs array.

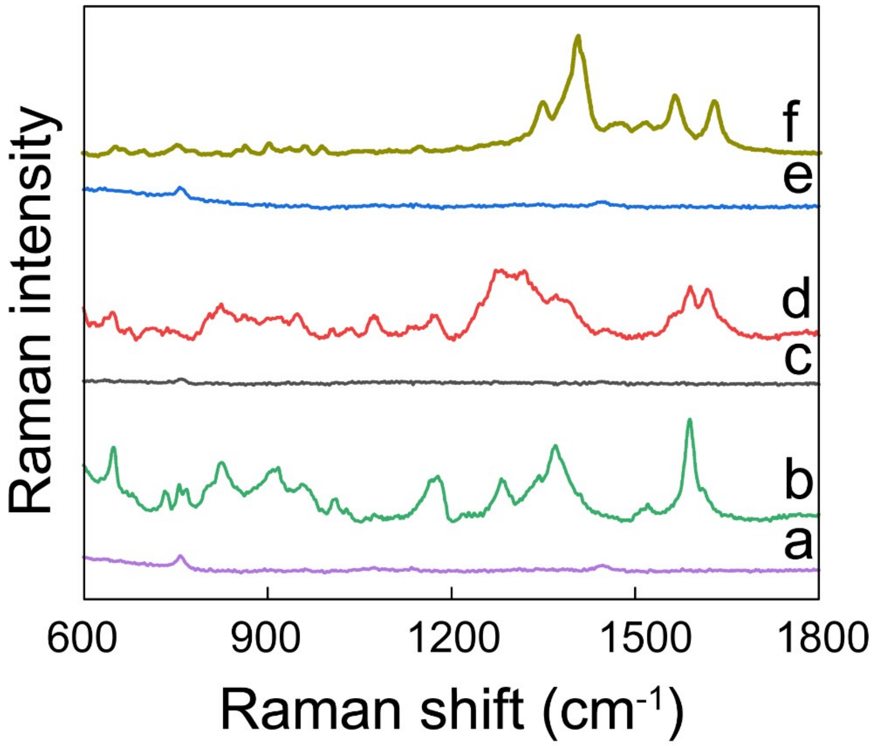

Fig. S9 SERS spectra of AgNPs/GNRs array (a), SERS spectrum of 10^{-6} M AM collected from the AgNPs/GNRs array (b) (the electrodeposition time of silver is 2 min), then the nanoarrays were stripped off and followed by silver electrodeposition for 2 min (c), and treated with the 10^{-6} M TC (d) (the electrodeposition time of silver is 2 min), then the nanoarrays were stripped off and followed by silver electrodeposition for 2 min (e), and treated with the 10^{-6} M OFX(f).

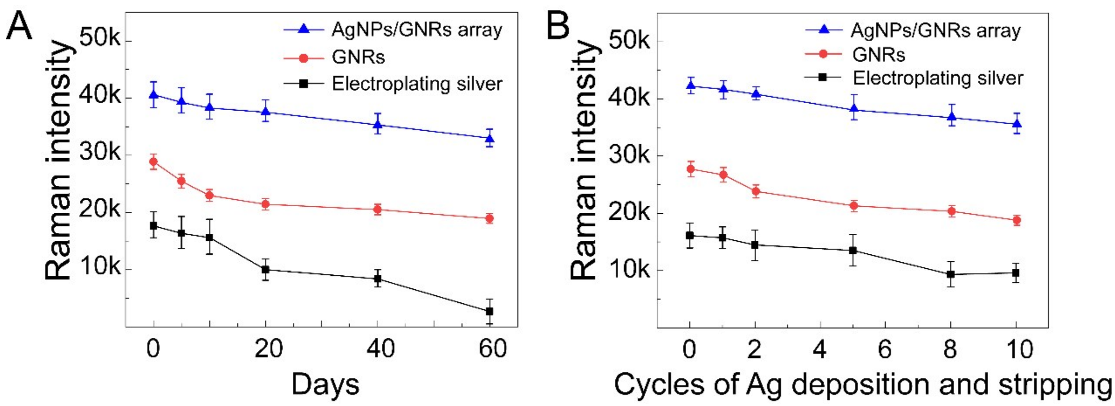

Fig. S10 (A) SERS intensity at 1080 cm^{-1} demonstrate the long-term stability of GNRs, electrodeposited AgNPs, and the AgNPs/GNRs array, respectively. (B) SERS intensity at 1080 cm^{-1} investigation of the recyclability of GNRs, electrodeposited AgNPs, and the AgNPs/GNRs array after 1~10 electrodeposition/stripping Ag cycles. The error bars represent typical intensity variations obtained from the same sample measured at 5 different spots.

Table S1. Comparing the detection performance of different methods for antibiotics analysis.

Methods	Materials[b]	Antibiotics	Linearity(μM)	LOD(μM)	References
Electrochemistry	MIP	Amoxicillin	1.6-1000	1.6	6
Electrochemistry	MWCNTs/CPE	Sulfapyridine	6×10^{-3}-1.61×10^{-1}	4.9×10^{-3}	7
ECL[a]	GE/H_2O_2/CTAB	Amoxicillin	4.32×10^{-2}-0.1	1.2×10^{-2}	8
Colorimetry	AuNPs	Tetracycline	4.58×10^{-1}-1	4.58×10^{-2}	9
Colorimetry	AuNPs	Amoxicillin	0.3-4.5	0.15	10
Fluorescence	Mn-doped ZnS QDs	Sulfonamide	0.5-80	0.5	11
Fluorescence	AuNPs/MBs	Ampicillin	2.48×10^{-4}-2.48	1.68×10^{-4}	12
SERS	MWCNTs-AuNPs	Sulfonamide	4×10^{-2}-4×10^{-1}	3.5×10^{-2}	13
SERS	(3D) ZnO/Ag@Au substrate	Sulfapyridine	10^{-3}-1	10^{-3}	14
SERS	PDMS-Ag	Amoxicillin	2.4×10^{-3}-2.4	2.4×10^{-3}	15
SERS	AgNPs/GNRs arrays	Amoxicillin	1.5×10^{-5}-200	0.5×10^{-5}	this work

[a]Electrochemiluminescence
[b]Abbreviations used: AMO-MIP QCM molecularly imprinted polymer and quartz crystal microbalance to detect amoxicillin; MWCNTs/CPE multi-walked carbon nanotubes modified carbon paste electrode; GE/H_2O_2/CTAB Graphite Electrode Hydrogen peroxide and cetyltrimethyl ammonium bromide; Aptamer-AuNPs the reaction between TC and aptamer lead to an aggregate of gold nanoparticles; AuNPs aggregation of citrate-capped gold nanoparticles; Mn-doped ZnS QDs: Mn-doped ZnS quantum dots; AuNPs/MBs gold nanoparticles modified magnetic bead composites; MWCNTs-AuNPs multi-walled carbon nanotubes and gold nanoparticles; (3D) ZnO/Ag@Au substrate three-dimensional structure of ZnO gold and silver substrate; PDMS-Ag polydimethylsiloxane silver dendrite.

Table S2. Experimental Raman shifts (cm^{-1}) of amoxicillin (AM) [16].

Experimental results /cm^{-1}	Documented in the literature /cm^{-1}	Assignment
840	846	in-plane deformation in C-H
1010	994	bending in NH_2
1040	1046	stretching in NH_2 and C-H
1177	1172	C-H bendiing in NH_2
1243	1266	in-plane deformation in benzene
1375	1392	twisting in NH_2
1463	1461	asymmetric bending in N-H
1611	1616	stretching in benzene ring
1780	1782	bending in CH_3

Table S3. Experimental Raman shifts (cm^{-1}) of tetracycline (TC) [17].

Experimental results /cm^{-1}	Documented in the literature /cm^{-1}	Assignment
818	747	stretching and out of plane swing in NH
947	888	bending in C-C
1078	1133	stretching in C-O
1174	1175	stretching in C-O
1277	1283	stretching and out of plane swing in NC
1318	1347	bending in C-H
1463	1459	bending and out of plane swing in CH_3
1590	1560	stretching in C=O
1618	1619	stretching and out of plane swing in COO^-

Table S4. Experimental Raman shifts (cm^{-1}) of ofloxacin (OFX) [18].

Experimental results /cm^{-1}	Documented in the literature /cm^{-1}	Assignment
1350	1353	bending in C-C and stretching in C-H
1405	1400	stretching in COO-
1565	1542	stretching in C=O
1628	1627	stretching in C=C

Table S5. Determination of antibiotics in seawater samples and comparison with HPLC-MS method.

Analytes	Spiked (μM)	This method Found (μM)	This method R[b] (%)	This method RSD (%)	HPLC-MS method Found (μM)	HPLC-MS method R (%)	HPLC-MS method RSD (%)
Amoxicillin	0.0	ND[a]	—	—	ND	—	—
	10	10.32	91.69	11.2	11.82	98.94	6.9
	50	47.93	95.84	9.4	52.75	97.69	7.3
Tetracycline	0.0	ND[a]	—	—	ND	—	—
	10	9.56	93.71	12.4	10.14	102.27	7.1
	50	56.48	94.23	10.8	51.34	97.54	7.7
Ofloxacin	0.0	ND[a]	—	—	ND	—	—
	10	11.89	92.32	12.6	12.84	99.63	8.2
	50	55.65	94.47	10.1	50.62	96.43	7.6

[a] ND: lower than LOD

[b] R: recovery of the method

References

1 P. Wang, L. Wu, Z. Lu, Q. Li, W. Yin, F. Ding, H. Han, *Anal. Chem*., 2017, **89**, 2424-2431.

2 F. Shao, Z. Lu, C. Liu, H. Han, K. Chen, W. Li, J. Chen, *ACS Appl. Mater. Inter*., 2014, **6**, 6281-6289.

3 X. Hu, T. Wang, L. Wang, S. Dong, *J. Phys. Chem. C*, 2007, **111**, 6962-6969.

4 K. Kim, J. Yoon, *Phys. Chem. B*, 2005, **109**, 20731-20736.

5 http://www.chemicalland21.com, 2007.

6 A. G. Ayankojo, J. Reut, R. Boroznjak, A. Öpik, V. Syritski, *Sens. Actuators B Chem*., 2018, **258**, 766-774.

7 S. M. Ghoreishi, M. Behpour, A. Khoobi, S. Masoum, *Arab. J. Chem*., 2017, **10**, 3156-3166.

8 L. Shen, H. Wang, P. Chen, C. Yu, Y. Liang, C. Zhang, *J. Food Drug Anal*., 2016, **24**, 199-205.

9 L. He, Y. Luo, W. Zhi, P. Zhou, *Food Anal. Methods*, 2013, **6**, 1704-1711.

10 M. Akhond, G. Absalan, H. Ershadifar, *Spectrochim. Acta A*, 2015, **143**, 223-229.

11 Y. Hu, X. Li, J. Liu, M. Wu, M. Li, X. Zang, *Anal. Methods,* 2018, **10**, 884-890.

12 Z. Luo, Y. Wang, X. Lu, J. Chen, F. Wei, Z. Huang, C. Zhou, Y. Duan, *Anal. Chim. Acta*, 2017, **984**, 177-184.
13 V. Moreno, A. Adnane, R. Salghi, M. Zougagh, Á. Ríos, *Talanta*, 2018, **194**, 357-362.
14 Y. Zhai, Y. Zheng, Z. Ma, Y. Cai, F. Wang, X. Guo, Y. Wen, H. Yang, *ACS Sens*., 2019, **4**, 2958-2965.
15 L. Wang, G. Zhou, X. Guan, L. Zhou, *Spectrochim. Acta A*, 2020, **235**,118-262.
16 G. Kibar, A. E. Topal, A. Dana, A. Tuncel, *J. Mol. Struct*., 2016, **1119**, 133-138.
17 L. Qu, Y. Liu, M. Liu, G. Yang, D. Li, H. Li, *ACS Appl. Mater. Inter*., 2016, **8**, 28180-28186.
18 M. R. El-Zahry, B. Lendl, *Spectrochim. Acta A*, 2018, **193**, 63-70.